Food Science of Animal Products

Research Article

Heat-induced oxidation and proteomic changes to yak milk protein

Jinchao Zhang[1,§], Yu Zhang[2,§], Rong Jing[1], Senbiao Shu[1], Jie Yang[1], Liang Li[1,3], Wenhan Wang[4] ✉, Zhendong Liu[1,3] ✉

[1] *Tibet Agriculture & Animal Husbandry University, Nyingchi 860000, China*
[2] *College of Food Science and Nutritional Engineering, China Agricultural University, Beijing 100083, China*
[3] *The Provincial and Ministerial Co-founded Collaborative Innovation Center for R&D in Tibet Characteristic Agricultural and Animal Husbandry Resources, Tibet Agriculture & Animal Husbandry University, Nyingchi 860000, China*
[4] *National Engineering Research Center of Edible Fungi, Key Laboratory of Applied Mycological Resources and Utilization of Ministry of Agriculture, Shanghai Key Laboratory of Agricultural Genetics and Breeding; Institute of Edible Fungi, Shanghai Academy of Agricultural Sciences, Shanghai 201403, China*
[§] These authors contributed equally to this work.
✉ Address correspondence to Wenhan Wang, wangwenhan@saas.sh.cn; Zhendong Liu, liu304418091@126.com
Received: April 7, 2024; Revised: April 15, 2024; Accepted: May 7, 2024

Abstract: Yak milk is a dietary source of high-quality protein in the plateau region of China but as yet uncharacterized oxidative changes occur during heat treatment. Therefore, oxidation of and proteomic changes to milk proteins from plateau pasture-fed yaks after at different temperatures were investigated. Content of carbonyl groups, surface hydrophobicity increased, and total sulfhydryl, disulfide bond content decreased. Endogenous fluorescence intensity decreased after at increasing temperatures, indicating increased particle size, and absolute values of the zeta potential decreased. Analysis by Fourier transform infrared spectroscopy showed changes of the secondary structure, with relative content of α-helices increasing and then decreasing, β-sheet showed a trend of decreasing and then increasing while the relative content of random curl did not change. The close range of the β-turn gradually decreased, breaking the protein microstructure, and folding stacking occurred. Proteomics analyses showed a temperature dependent effect. Sixty-two proteins were suppressed and 49 elevated with 4 pathways up-regulated and 7 down-regulated at 65 °C. Thirty-one proteins were suppressed and 37 elevated with 5 pathways up-regulated and 4 down-regulated at 90 °C. The most extensive changes were observed at 120 °C, when 327 proteins were suppressed and 308 elevated with 11 pathways up-regulated and 33 down-regulated.

Keywords: yak milk; protein; oxidation; heat treatments; proteomics; structure

Citation: J. C. Zhang, Y. Zhang, R. Jing, et al., Heat-induced oxidation and proteomic changes to yak milk protein, Food Sci. Anim. Prod. 2 (2024) 9240056. https://doi.org/10.26599/FSAP.2024.9240056.

1 Introduction

Yak milk is a primary source of high-quality protein for the inhabitants of the highland regions of China and represents an economically significant industry. Heat treatment is a necessary part of processing in the form of low- or high-temperature pasteurization and ultra-high-temperature. The high content of unsaturated lipids, endogenous oxidative enzymes, metal catalysts and other components could potentially cause that oxidative damage occurs during heat treatment[1–2]. High temperature, high pressure and shear conditions cause breakage of the peptide chain[3], protein aggregation or cross-linking[4], formation of carbonyl groups and loss of free amino acids[5]. Physical properties are also affected by oxidation, such as solubility, hydrophobicity, water retention and antioxidant capacity. Native protein function may be completely lost as a result[6]. Fats may also be oxidized, generating fatty oxygenates, such as malondialdehyde, to accelerate oxidation, denaturation and cross-linking of proteins[7–8]. Such changes may decrease the nutritional value of dairy products and have health implications. Incorrect degradation, folding and accumulation of oxidation products may lead to oxidative stress and imbalance of the redox state. Such effects have been linked to atherosclerosis[9–10], diabetes mellitus and neurological weakness[11], among other disease states. Addition of protein oxides to the diet of mice has been found to cause oxidative damage to the liver, kidneys and digestive organs and to activate the JNK/p38/TGF-β1 signaling pathway to induce oxidative stress, inflammation and renal fibrosis[12–14]. In addition, oxidized tyrosine products caused apoptosis of mouse islet and MIN-6 cells and changes to thyroid hormone levels[15–17]. We hypothesized that oxidative modifications to yak milk caused by heat treatment would alter absorption of oxidation products and affect health status. Conventional biochemical methods are limited to identifying changes to specific proteins but 4D off-label proteome quantification technology improves proteomic analysis with increased speed.

Proteomics is a relatively new field which enables precise analysis of complex dairy protein mixtures, including protein detection, identification, characterization and quantification. Proteomics

technology has been used to analyze proteomic differences in milk fat globule membrane proteins from human, bovine, goat and yak sources[18] and identify and quantify 198, 169, 213 and 128 proteins respectively in the respective sera[19]. Proteomics techniques also allowed identification of 2 650 proteins in yak *longissimus thoracis*, revealing that phosphoproteins were involved in myogenic fiber organization, energy metabolism regulation and signaling and *N*-glycoproteins in extracellular matrix organization, cellular immunity and organic matter homeostasis *in vivo*[20]. One hundred and eighteen out of 181 *N*-glycoproteins were identified in milk and yogurt and 13 *N*-glycosyl groups were found to be significantly changed following fermentation[21]. Signaling interactions during neonatal immunity and digestive maturation have also been elucidated[22–23]. However, protein modifications in heat-treated yak milk have not previously been analyzed. The current study investigated protein oxidation in yak milk from the Tibetan plateau after at different temperatures to inform processing methodologies.

2 Materials and methods

2.1 Materials

Fresh yak milk was collected from the plateau pasture in Dangxiong County, Lhasa City, Tibet in June 2021 and transported to the laboratory at –4 °C.

Aniline-1-naphthalenesulfonic acid (ANS), disodium hydrogen phosphate, potassium dihydrogen phosphate, 2,4-dinitrophenylhydrazine (DNPH), sodium dodecyl sulfate (SDS), 5,5'-dithiobis(2-nitrobenzoic acid) (DTNB), trichloroacetic acid (TCA), guanidine hydrochloride, ethanol, ethyl acetate, Coomassie brilliant blue R-250, sodium hydroxide, potassium chloride, hexa magnesium chloride dihydrate, calcium chloride dihydrate, hydrochloric acid, ammonium carbonate, sodium bicarbonate, sodium chloride, glutaraldehyde, disodium hydrogen phosphate and sodium dihydrogen phosphate were purchased from Chengdu Kolon Chemical Co.

2.2 Sample preparation

Yak milk samples were centrifuged at 2 149 × *g*, 4 °C for 15 min. The upper fat layer discarded and the lower liquid layer (whey protein) retained. Samples were divided into 4 groups: control, low temperature pasteurization (65 °C for 30 min), high temperature pasteurization (90 °C for 10 min) and high temperature group (120 °C for 10 min). Sterilized samples were freeze-dried at –50 °C.

2.3 Measurement of the base content

Assays were performed according to the methods of Mestdagh et al.[24] and Shao et al.[25] with slight modifications. Briefly, 0.2 mL diluted sample solution was added to 0.8 mL HCl (2 mol/L) containing 10 mmol/L DNPH and mixed with 2 mol/L HCI without DNPH used as a blank. Solutions were incubated for 1 h at room temperature. Then 0.4 mL 40 g/100 mL TCA added with mixing and standing for 30 min. The precipitate was centrifuged at 10 000 r/min for 20 min at 4 °C, washed 3 times with ethanol-ethyl acetate (1:1, *V*/*V*) and dissolved in 1.0 mL phosphate buffer (0.02 mol/L, pH 6.5) containing 6 mol/L guanidine hydrochloride. Absorbance was measured at 370 nm and carbonyl content was expressed as nmol DNPH/mg protein (molar extinction coefficient = 22 000 L/(mol·cm)). Protein content was determined by BCA kit and calculated by Eq. (1):

$$\text{Protein carbonyl content (nmol/mg)} = \frac{OD_1 - OD_2}{22 \times L \times \rho} \times 125 \times 10^5 \quad (1)$$

Where OD_1 is the absorbance of the test tube, OD_2 is the absorbance of the control tube, L is the colorimetric optical diameter (10 mm), and ρ is the protein concentration in the sample (mg/mL).

2.4 Determination of sulfhydryl content and disulfide bonds

Free and total sulfhydryl groups were determined by DTNB colorimetric assay according to the methods of Cao et al.[26] and Wang et al.[27] with slight modifications.

Free sulfhydryl groups: 0.5 mL sample was mixed with 2.0 mL SDS solution (0.03 g/mL) and 0.2 mL DTNB (10 mmol/mL) was added with incubation for 1 h of light-proof reaction and the absorbance was measured at 412 nm. DTNB-free solution was used as the control and free sulfhydryl content in mmol/g prot was calculated according to the following formula.

Total sulfhydryl groups: 0.8 mL defatted sample was mixed with 0.2 mL 8 mol/L urea and 0.03 g/mL SDS solution for 1 h before 0.5 mL 40 g/100 mL TCA solution was added with incubation for 1 h. Samples were centrifuged at 5 000 r/min for 10 min. The precipitate washed with 40 g/100 mL TCA and centrifugation repeated. The process was repeated twice and the final precipitate dissolved in 1 mL SDS solution (0.03 g/mL). Total sulfhydryl content was determined as above for free sulfhydryl content.

Disulfide bond content was calculated from total sulfhydryl content minus free sulfhydryl content divided by 2. Results are calculated by Eq. (2) and expressed as sulfhydryl content per mg of protein (nmol/mg):

$$\text{Sulfhydryl content (nmol/mg)} = 73.53 \times A_{412\,\text{nm}} \times \frac{D}{\rho} \quad (2)$$

Where $A_{412\,\text{nm}}$ is the absorbance of the sample after subtracting the reagent blank, D is the dilution factor, and ρ is the protein concentration (mg/mL).

2.5 Fourier transform infrared (FTIR) spectroscopy analysis

Samples were lyophilized and 2 mg aliquots mixed with 200 mg KBr by grinding for 1 min at room temperature in a dry environment to produce transparent flakes which were scanned by FTIR spectrometry under the following conditions: range of scanning wave number: 400–4 000 cm^{-1}, resolution: 4 cm^{-1}, number of scans: 64 with baseline correction, smoothing, Fourier self-deconvolution, peak fitting (Gaussian formula with half-peak width of 1.5 nm) performed by OMINC software. Relative content of secondary structure was calculated from the peak area of the fitted peaks and Origin 8 software used for plotting.

2.6 Determination of particle size and zeta potential

Samples were diluted with distilled water to give a final protein concentration of 0.3 to 0.6 mg/mL. Mean particle size and zeta potential were determined using a nano-laser particle size meter. Measurements were made in triplicate.

2.7 Microstructure observation

Scanning electron microscope (SEM) analysis was performed by diluting samples (1:6) with deionized water, placing 100–200 μL on coverslips and freezing in liquid nitrogen before gold spraying in a vacuum coating device[28]. Samples were observed under a SEM (GeminiSEM 560, Japan) at a resolution of 20 μm with magnification 500 ×.

2.8 Endogenous fluorescence determination

Samples were diluted to 0.1 mg protein/mL with 0.01 mol/mL phosphate buffer (pH 7.0). The excitation wavelength of the fluorescence spectrophotometer was set to 283 nm and emission wavelength was scanned in the 300–500 nm range at a scanning speed of 300 nm/min. Excitation and emission slit widths were 5 nm. Scans were performed in triplicate at room temperature.

2.9 Determination of surface hydrophobicity

Samples were diluted to give final protein concentrations of 0.1, 0.2, 0.4, 0.6, 0.8 and 1.0 mg/mL with 0.01 mol/mL phosphate buffer (pH 7.0). First, 20 μL ANS solution (8 mol/mL) was added with mixing and incubation for 3 min at room temperature in the dark. Samples were scanned in the 300–500 nm range with an excitation wavelength of 283 nm and a scanning speed of 300 nm/min. Excitation and emission slit widths were 5 nm and samples were scanned in triplicate. Protein concentration was plotted against fluorescence intensity to give a gradient which represents the protein's surface hydrophobicity index (S_0).

2.10 Proteomic analysis

Protein extraction: frozen sample powder was added to 4 volumes of lysis buffer (containing 8 mol/L urea, and 1% protease inhibitor) and lysed by ultrasonic waves, centrifuged at 12 000 × *g*, 4 °C, for 10 min and protein concentration of the supernatant determined using BCA kit.

Trypsin digestion: equal amounts of sample protein were suspended in equal volumes of lysis solution and 20 g/100 mL TCA added slowly with mixing and incubation for 2 h at 4 °C to allow precipitation. Samples were centrifuged at 4 500 × *g* for 5 min, the supernatant discarded and the precipitate washed 2–3 times with pre-chilled acetone. The precipitate was dried, 200 mmol/L final concentration of triethanolamine buffered saline added and sonication performed. Trypsin was added in a ratio of 1:50 (protease: protein, *m*/*m*) and allowed to digest overnight. 5 mmol/L dithiothreitol was added and incubated for 30 min at 56 °C before addition of 11 mmol/L iodoacetamide with incubation for 15 min at room temperature in the dark.

Liquid chromatography-mass spectrometry analysis: peptides were dissolved in liquid chromatography mobile phase A (0.1% formic acid and 2% acetonitrile in water) and separated using an EASY-nLC 1200 ultra-performance liquid chromatography system. Mobile phase B was 0.1% formic acid and 90% acetonitrile in water. Liquid phase gradient settings were: 0–26 min, 9%–25% B; 26–34 min, 25%–35% B; 34–37 min, 35%–80% B; 37–40 min, 80% B with flow rate of 500 nL/min. Separated peptides were injected into the NanoSpray ionization source and then into the Orbitrap Exploris™ 480 mass spectrometer for analysis of peptide parent ions and their secondary fragments. Ion source voltage was 2.2 kV, and FAIMS compensation voltage (CV) was –45 and –70 V. Primary mass spectrometry scan range was 400–1 500 *m*/*z* and scan resolution was 60 000; secondary mass spectrometry scan range was 100 *m*/*z* and secondary scan resolution was 15 000 with TurboTMT off. A data-dependent scanning program was used to identify the top 20 peptide ions with the highest signal intensities after the primary scan. Peptide parent ions were sequentially entered into the high energy collision dissociation collision cell using 28% fragmentation energy for fragmentation and the same sequential secondary mass spectrometry performed. Automatic gain control was 5×10^4, signal threshold was 2×10^4 ions/s, maximum injection time was 100 ms and dynamic exclusion time of the tandem mass spectrometry scan was 30 s to avoid repeated scanning of parent ions[29–33].

2.11 Statistical analyses

SPSS 25.0 software was used to perform an independent sample Tukey's test. A value of $P < 0.05$ was considered to indicate a significant difference and other data are presented as mean ± standard deviation (SD). OriginPro 2012 software was used for plotting.

3 Results

3.1 Oxidative index

Carbonyl derivative content indicates the extent of protein oxidation[34] and content compared to the control. Carbonyl content increases with temperature during the heating process (Figure 1A). Sulfhydryl groups may be free on the protein's surface or encapsulated within the protein[35]. Free sulfhydryl group content increased gradually with rise in temperature but the content at 65 and 90 °C was lower than that of the control group and higher in the 120 °C group (Figure 1B). Total sulfhydryl group content after all heat treatments, being more pronounced for the 65 °C samples ($P < 0.05$) and a smaller decrease for the 90 and 120 °C samples. Decreased sulfhydryl group content is an indication of protein oxidation, which is intensified at higher temperatures (Figures 1B and C). Disulfide bond content was similar in 65 and 120 °C samples and both were significantly lower than controls ($P < 0.05$) (Figure 1D).

3.2 FTIR spectrum

FTIR spectrum may be used to indicate changes of the secondary structure during protein oxidation[36]. Yak milk proteins have absorption bands in the infrared region in the range of 1 600–1 700 cm^{-1}, due to α-helix and β-sheet. A higher followed by a lower peak change can be seen for the yak milk protein FTIR spectra with increasing temperature (Figure 2A).

β-Sheet relative content decreased and then increased for the 65 and 90 °C groups and significantly increased for the 120 °C group (Figure 2B). Random coil relative content increased from 65 to 90 °C. No significant trend could be seen for α-helix relative content. 65 °C treatment decreased, 90 °C increased and 120 °C abolished α-helix relative content. β-Turn tended to increase and then decrease with increasing temperature, producing an increase at 65 °C and a decrease at 90 and 120 °C compared with controls. An orderly to disorderly transformation was achieved during heat treatment.

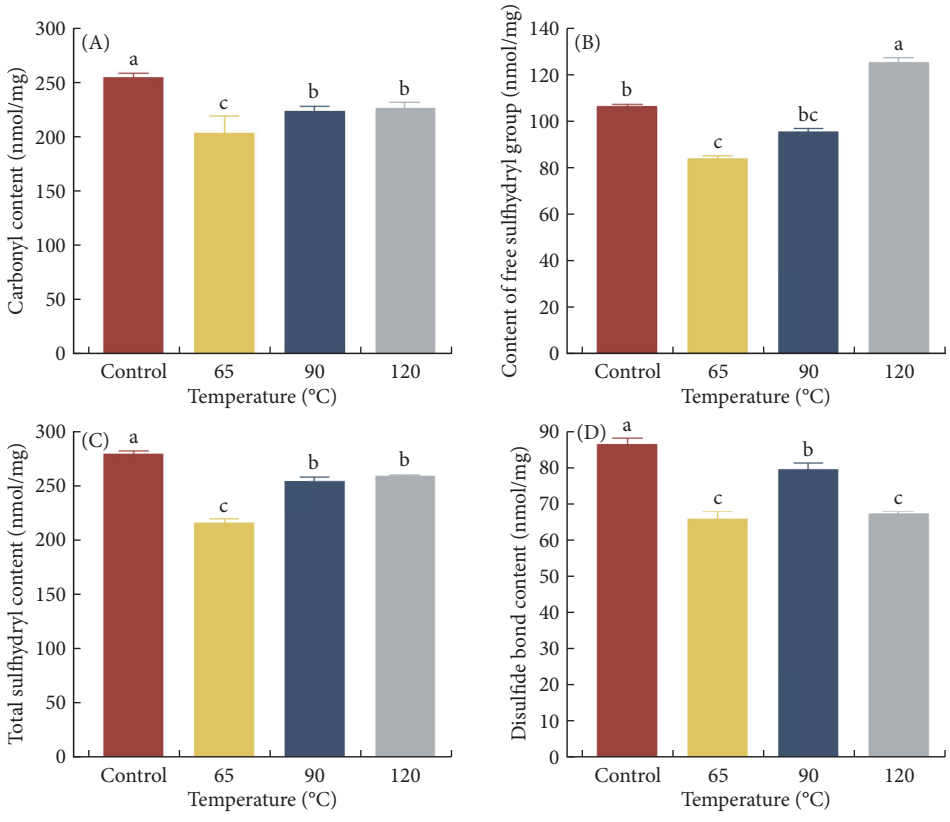

Figure 1 Changes in contents of (A) carbonyl, (B) free sulfhydryl, (C) total sulfhydryl, and (D) disulfide bond. Data are expressed as mean ± SD (n = 3). Superscript letters indicate significant differences by Tukey's test and one-way ANOVA ($P < 0.05$).

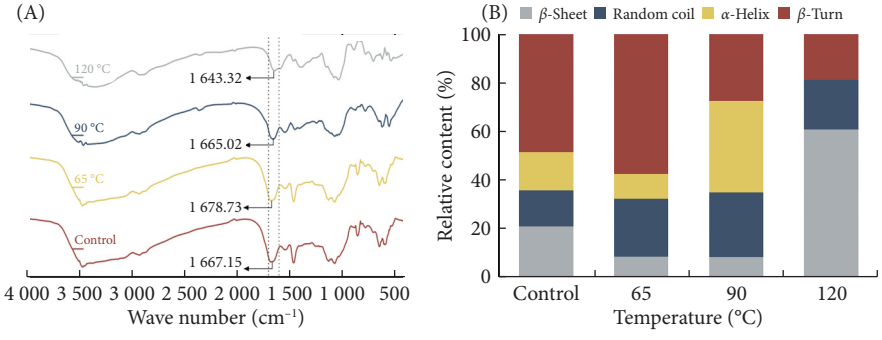

Figure 2 Changes of (A) FTIR spectra and (B) secondary structure of yak milk protein. Superscript letters indicate significant differences by Tukey's test and one-way ANOVA ($P < 0.05$).

3.3 Particle size and zeta potential

Mean particle size is a reflection of the aggregation of soluble proteins[37] and did not change significantly at 65 and 90 °C compared to controls but showed a significant increase at 120 °C ($P < 0.05$, Figure 3A). Zeta potential refers to the electric potential of the colloidal dispersion, a higher absolute value indicating greater stability of myogenic fibrin[38]. Absolute potential decreased gradually so that no significant changes were seen at 65 and 90 °C but decreased at 120 °C ($P < 0.05$) compared with controls (Figure 3B).

3.4 Surface microstructure

Changes to surface microstructure may be seen by SEM. Controls had flat and compact proteins but sieve-like holes and fractures were apparent at 65 °C and changes in curling, spiraling, folding and stacking at 120 °C (Figure 4).

3.5 Endogenous fluorescence and surface hydrophobicity

Endogenous fluorescence intensity decreased, at all temperatures and was most pronounced at 120 °C (Figure 5A). Structural and functional changes to proteins emphasize the roles of superficial hydrophobic interaction changes[39–40]. Hydrophobicity decreased at all temperatures ($P < 0.05$) producing a similar effect at 65 and 90 °C and being most significant at 120 °C (Figure 5B).

3.6 Proteomics analysis

3.6.1 *Protein identification and quantification*

Total spectra numbered 567 057 of which 66 370 were effective. Totally, 4 235 peptides were identified, of which 4 116 were unique, 1 230 proteins were resolved by specific peptide and 1 112 were quantified by specific peptide (Figure 6A). Most peptides consisted of 7–20 amino acids, in accordance with the general pattern of

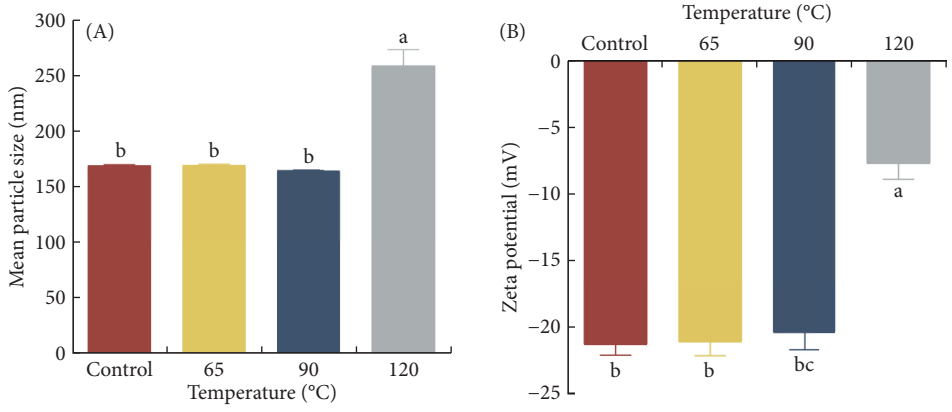

Figure 3 Variation of (A) mean particle size and (B) zeta potential. Data are expressed as mean ± SD (n = 3). Superscript letters indicate significant differences by Tukey's test and one-way ANOVA ($P < 0.05$).

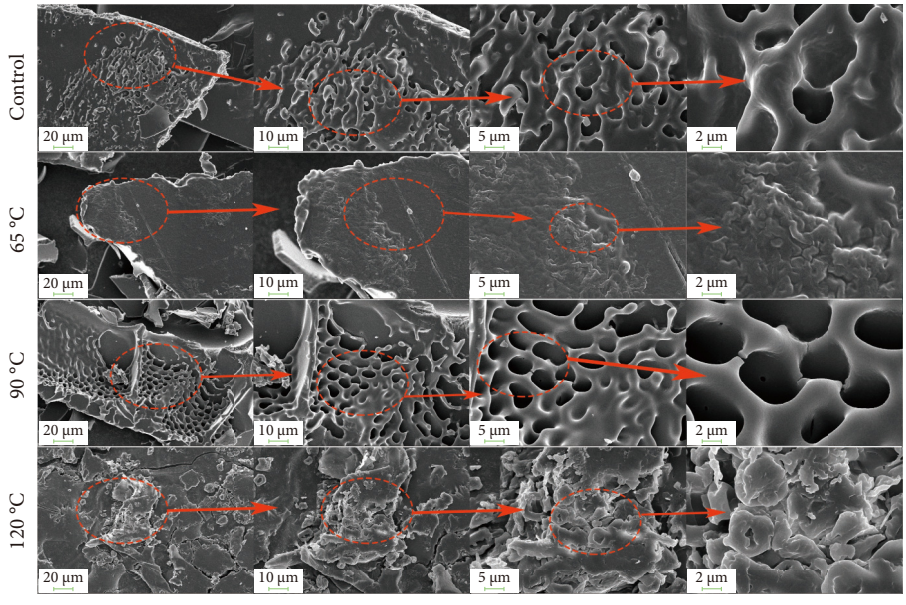

Figure 4 Scanning electron microscopy of yak milk protein.

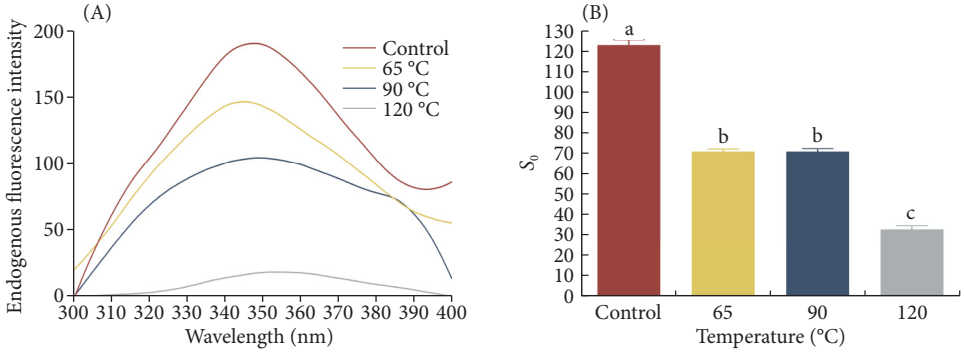

Figure 5 Variation of (A) endogenous fluorescence intensity and (B) hydrophobicity. Data are expressed as mean ± SD (n = 3). Superscripts indicate significant differences by Tukey's test and one-way ANOVA ($P < 0.05$).

enzymatic cleavage and mass spectrometry-based fragmentation (Figure 6B). The distribution of peptide lengths was within quality control limits (Figure 6E) and most proteins corresponded to more than 2 peptides. Molecular weights of the proteins identified were present in different phases and evenly distributed and were concentrated in the 10–70 kDa range (Figure 6F). Reproducibility of these results was tested by Pearson's correlation coefficient and relative standard deviation (RSD) (Figures 6C and D).

3.6.2 *Screening of differential proteins*

Functional variability was assessed in addition to the quantitative analysis (Figure 7A). After 120 °C, 327 proteins had reduced and 308 increased function. Sixty-two proteins had increased and 49 reduced function after 65 °C treatment and 31 had increased and 37 decreased function after 90 °C treatment. Volcano plots are shown in Figures 7B–D.

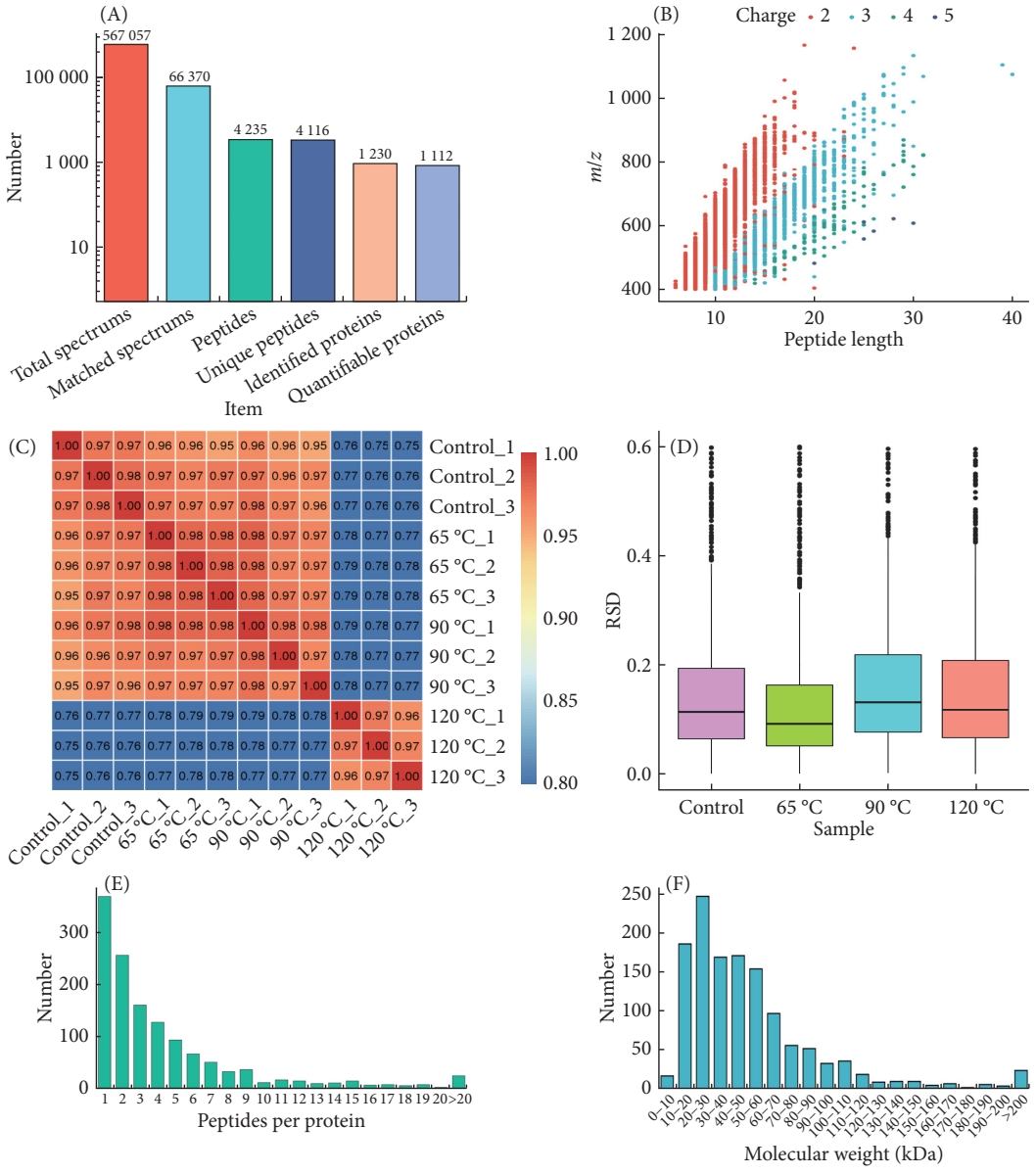

Figure 6 (A) Overview of protein identification. (B) Peptide length distribution. (C) Heat map of Pearson correlation coefficient. (D) Relative standard deviation (RSD) box line plot. (E) Peptide number distribution. (F) Molecular weight distribution.

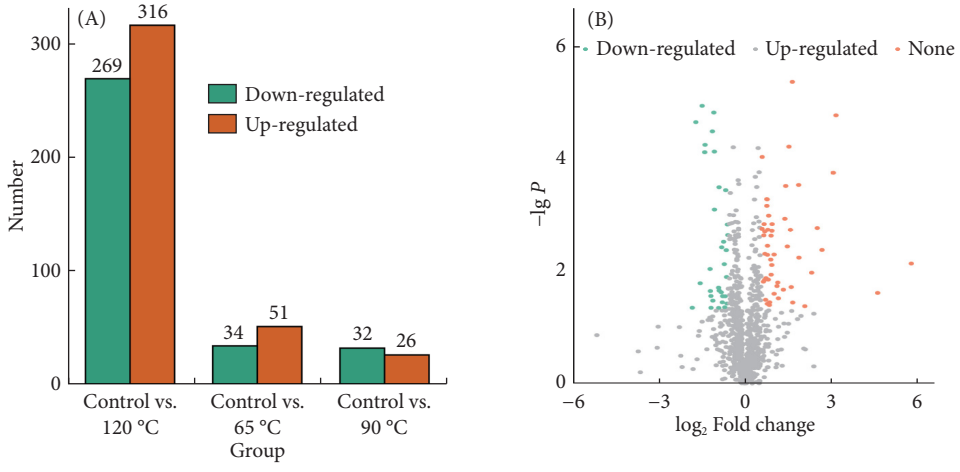

Figure 7 (A) Protein functions and volcano plots for (B) control vs. 65 °C, (C) control vs. 90 °C, and (D) control vs. 120 °C, respectively ($P < 0.05$).

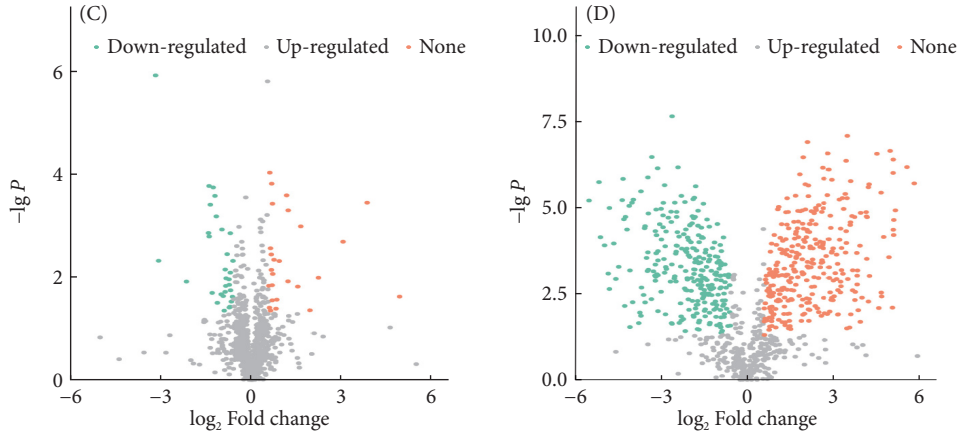

Figure 7 *(Continued)*

3.6.3 *Classification of protein function changes*

Gene ontology (GO) and clusters of orthologous groups of proteins/eukaryotic orthologous groups (COG/KOG) functional classification analyses of altered proteins were performed. GO analysis of biological process, cellular component and molecular function revealed that protein changes for all 3 groups were concentrated in cellular process, biological regulation and response to stimulus functions (Figure 8).

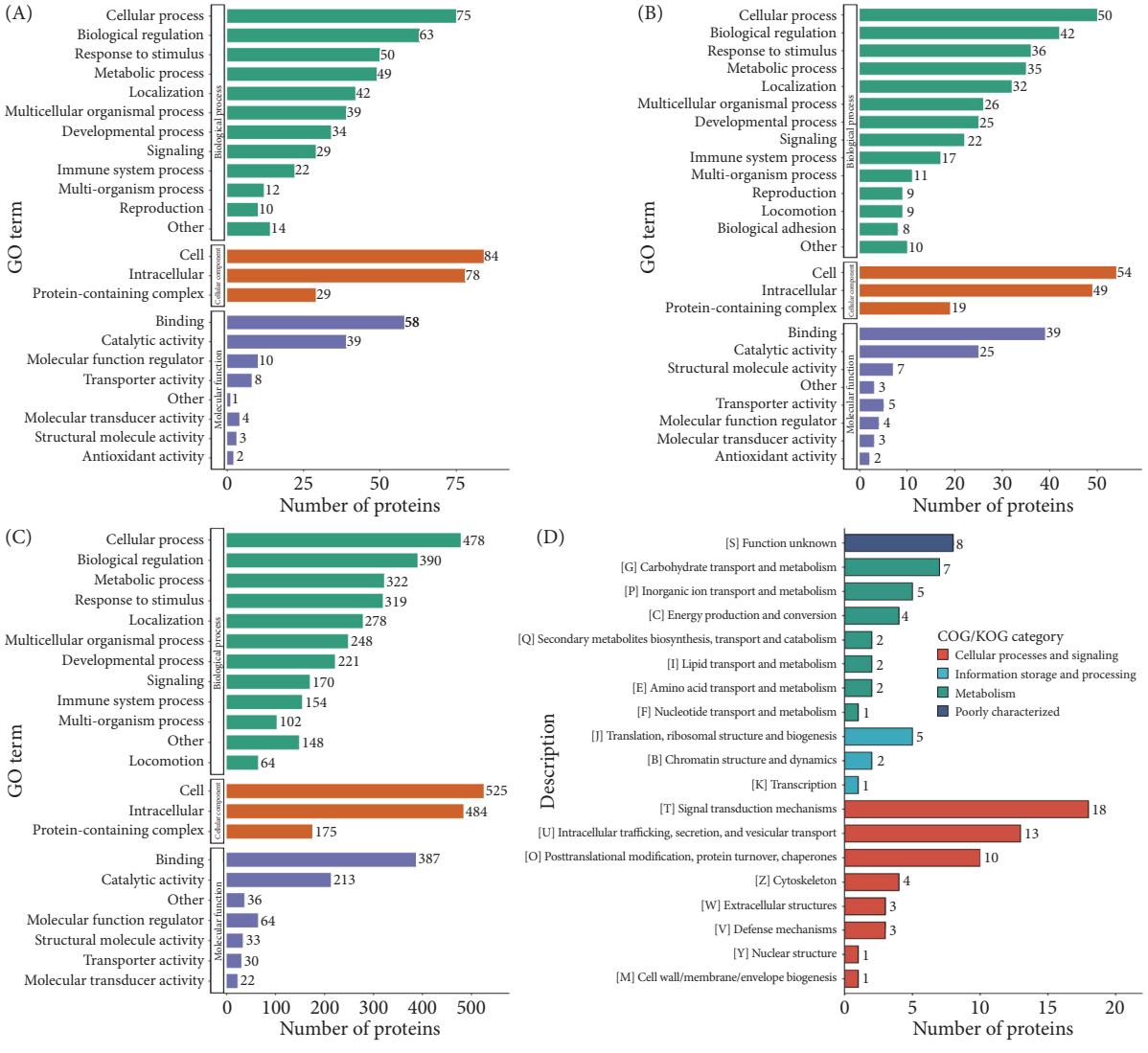

Figure 8 Gene ontology secondary annotation classification for (A) control vs. 65 °C, (B) control vs. 90 °C, and (C) control vs. 120 °C. COG/KOG functional classification for (D) control vs. 65 °C, (E) control vs. 90 °C, and (F) control vs. 120 °C.

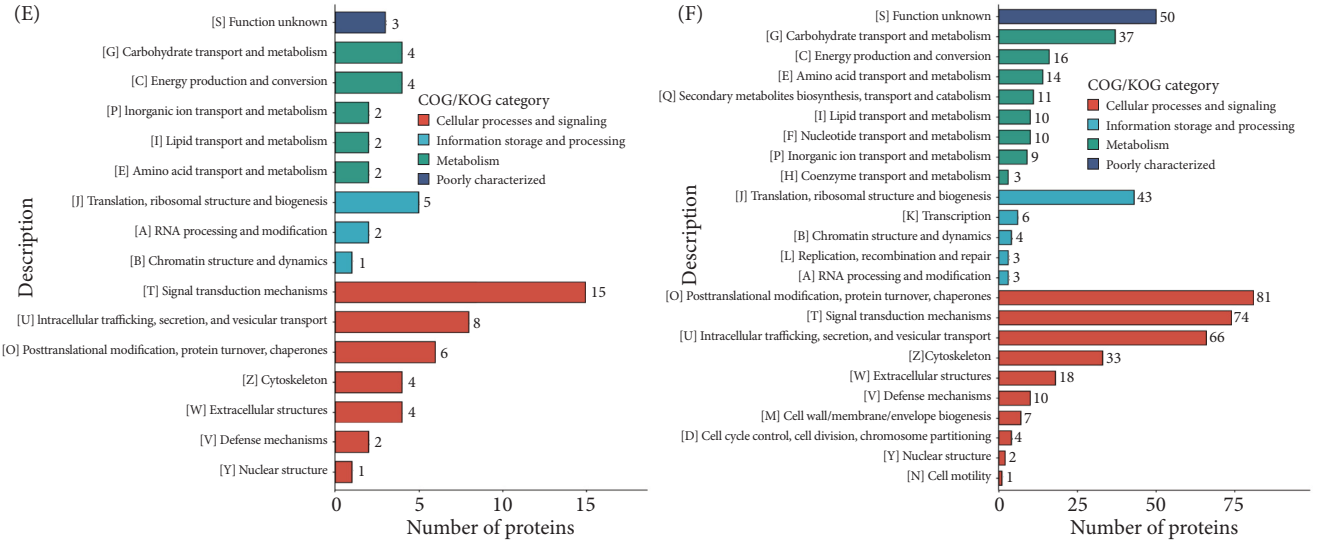

Figure 8 *(Continued)*

3.6.4 Kyoto Encyclopedia of Genes and Genomes (KEGG) enrichment pathway analysis

KEGG pathway analysis showed that changes impacted protein digestion and absorption. Four pathways were upregulated after 65 °C treatment, including oxidative phosphorylation and Hedgehog signaling and 7 were downregulated, including systemic lupus erythematosus (SLE) and prion disease (Figure 9). Treatment at 90 °C increased 5 pathways such as transcriptional misregulation in cancer, gastric cancer, arrhythmogenic right ventricular cardiomyopathy, and reduced 4 pathways, such as glycosaminoglycan degradation, epidermal growth factor receptor (EGFR) tyrosine kinase inhibitor resistance; moreover, PI3K-Akt signaling pathway, extracellular matrix (ECM)-receptor interaction, small cell lung cancer pathway was reduced or increased to varying degrees. 120 °C treatment upregulated 11 disease-related pathways, such as glycolysis/gluconeogenesis, transcriptional misregulation in cancer, primary immunodeficiency and so on, and downregulated 33 pathway, such as down-regulate oxidative phosphorylation, insulin signaling pathway and so on.

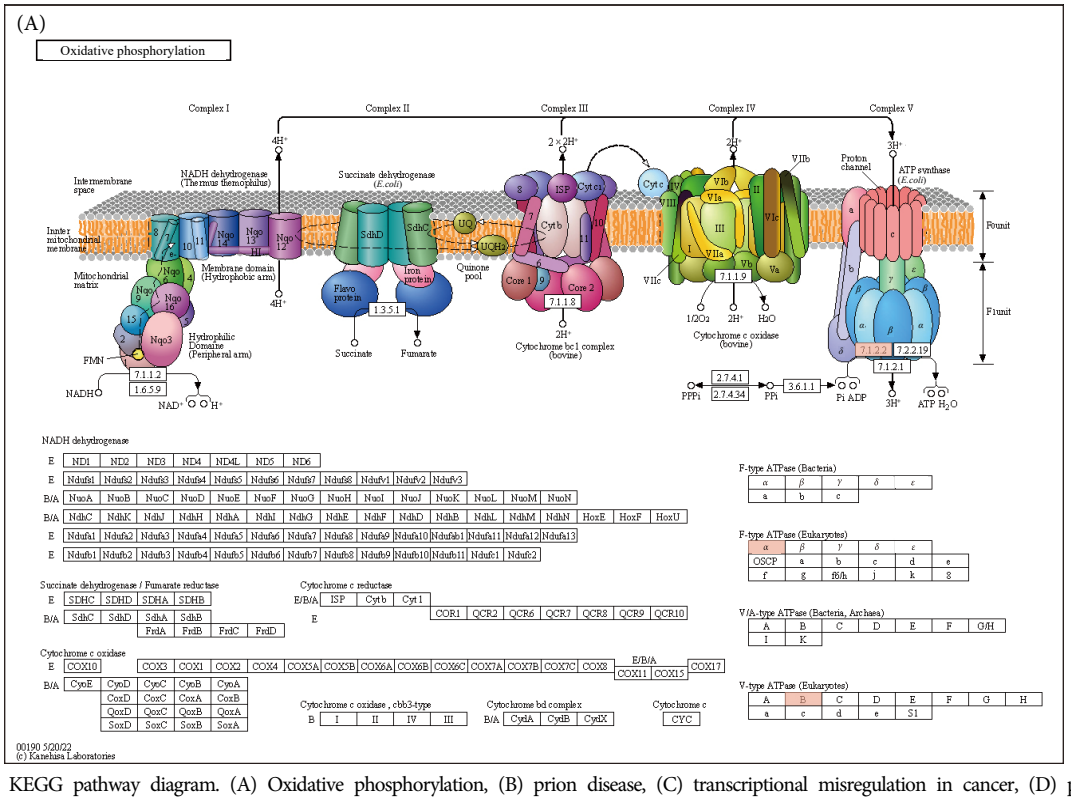

Figure 9 Partial KEGG pathway diagram. (A) Oxidative phosphorylation, (B) prion disease, (C) transcriptional misregulation in cancer, (D) proteasome, and (E) primary immunodeficiency. Red fill indicates differentially up-regulated proteins; green fill indicates differentially down-regulated proteins; yellow fill indicates that this node contains both differentially up-regulated and down-regulated proteins.

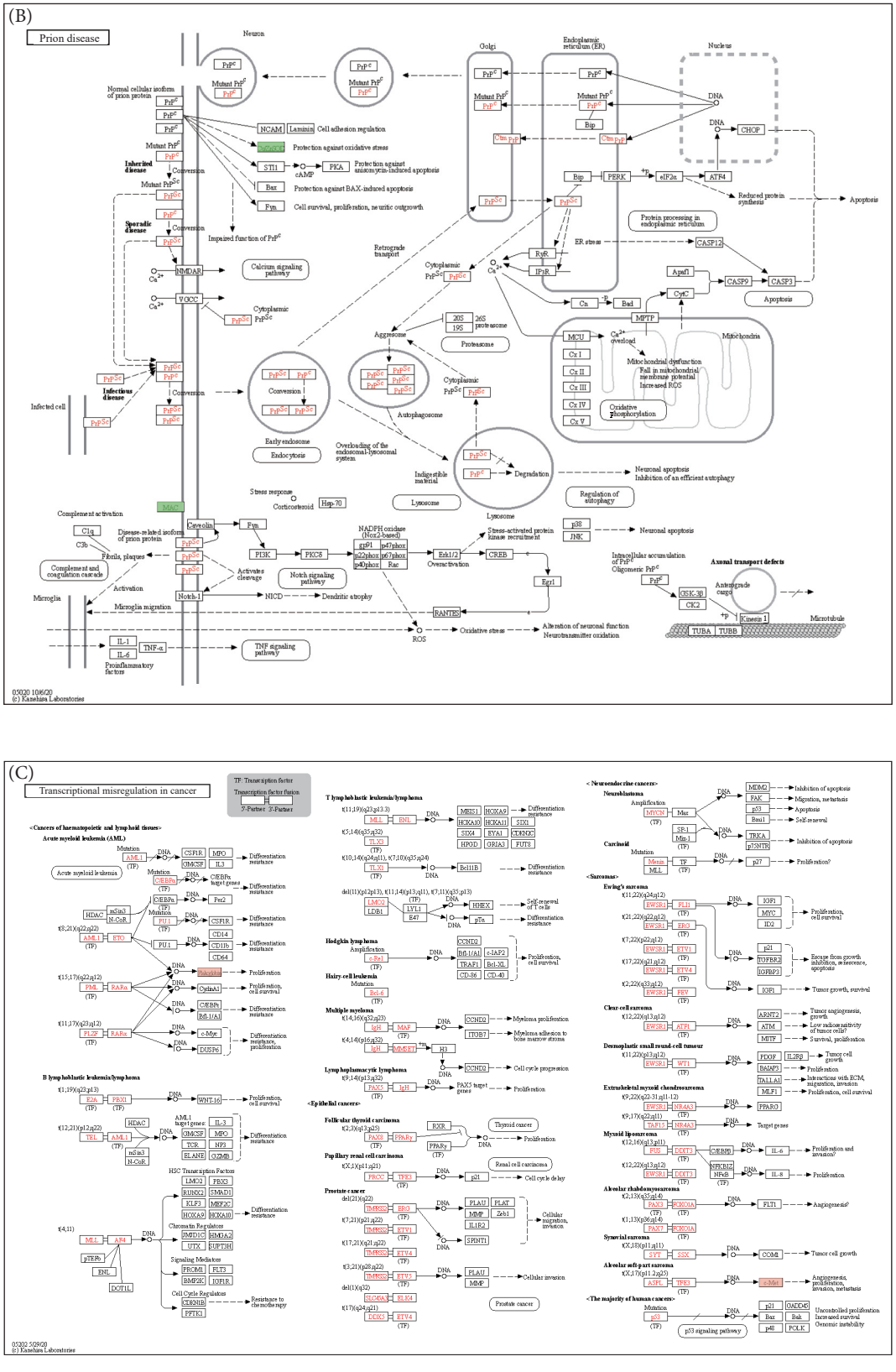

Figure 9 *(Continued)*

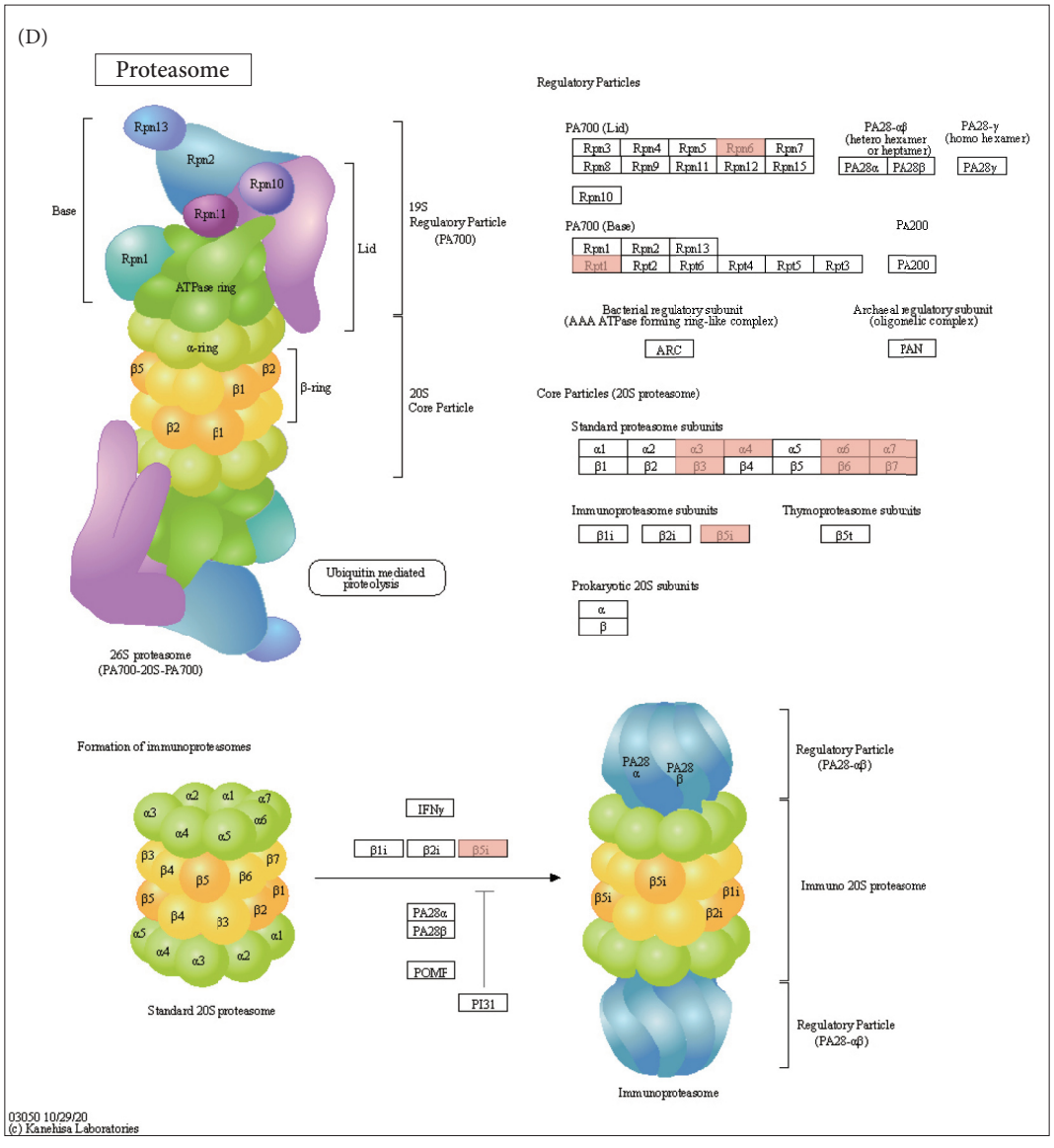

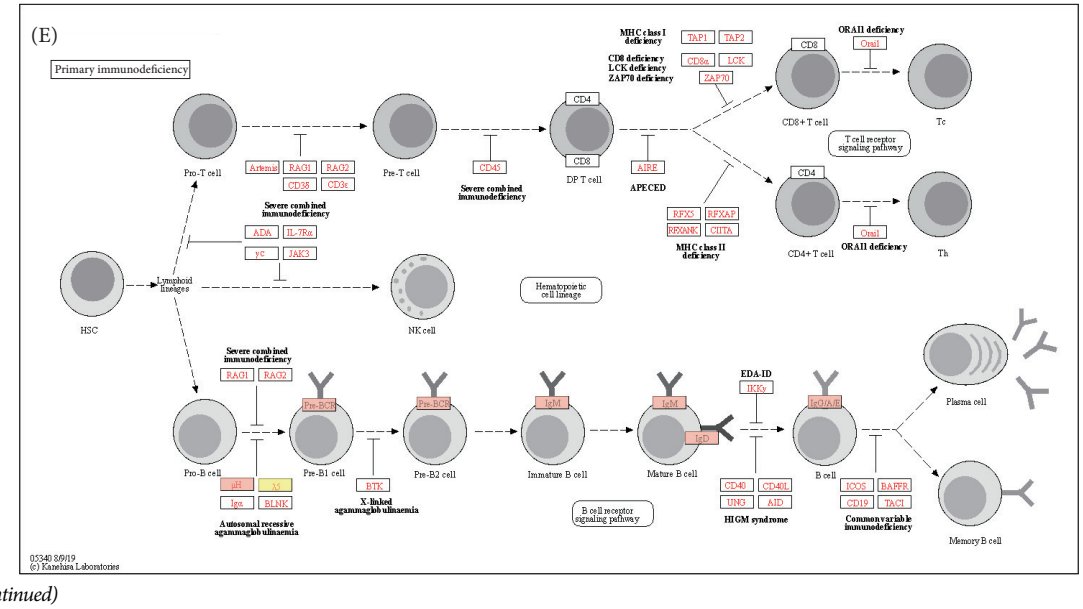

Figure 9 *(Continued)*

4 Discussion

Accumulation of oxidized proteins has been associated with chronic disease progression[39], an observation that has implications for heat treatment of yak milk. The current study relates the degree of oxidation to heat treatment temperature. Carbonyl content increased with increasing temperature; total and free sulfhydryl groups change, with potential adverse effects, such as taste changes, skin mucous membrane damage and immune complex membrane glomerulopathy caused by proteinuria and aspergillosis[41]. Changes in sulfhydryl groups reflect the may occurrence of oxidation reactions. Disulfide bonds are associated with protein higher structure and activity[42]. Disulfide bond content decreased after heat treatment which may cause higher structural changes, reducing biological activity. Endogenous fluorescence spectra indicated changes to the non-polarity of the microenvironment of tryptophan residues due to the formation of aggregates[26] and decreased endogenous fluorescence indicated changes to protein structure[43]. The occurrence of aggregation was shown by increased particle size after 120 ℃ treatment[37]. Higher temperatures may increase the degree of oxidation and promote the formation of insoluble fractions, leading to aggregation and reduced functional properties, such as water-holding[44]. Decreased absolute values of zeta potential at 120 ℃ may indicate a cohesive, aggregated state of proteins with reduced stability[45]. Hydrophobicity also decreased with increasing temperature, perhaps due to oxidation reactions causing the exposure of aromatic and aliphatic side chains to the polar environment. Insoluble aggregates formed through hydrophobic interactions lead to decreased surface hydrophobicity[46] and increased particle size. Increased surface hydrophobicity is known to strengthen and potentiate binding between proteins[47]. Decreased hydrophobicity found during the present study may lead to functional changes. Surface microstructural changes were also observed to increase with increasing temperature by SEM. FTIR results showed secondary structural alterations to proteins during heat treatment, and together with the microstructural changes, indicate that proteins were damaged with potential impact on function. The stability of protein secondary structure is strongly influenced by temperature, and high temperatures can lead to structural denaturation and inactivation of proteins. The reason for the decrease and then increase in the content of different secondary structures is not clear.

Proteomic analysis revealed that 327 proteins were increased and 308 decreased by 120 ℃, 62 were increased and 49 decreased at 65 ℃ and 31 increased and 37 decreased at 90 ℃. Biological processes, cellular components and molecular functions were all affected.

Oxidative damage usually impairs protein function. The current study found that at 65 ℃ achieved better preservation of the nutritional value of yak milk, such as the ability to increase the F-type H^+-ATPase during oxidative phosphonate transporting, the ability to accelerate body metabolism[48] and the ability to inhibit complement (C5) activation. C5 forms a periplasmic attack complex (C5b-9) or produces allergenic toxins in SLE and the cellular activator, C5a, causes tissue damage that attracts neutrophils and macrophages by releasing oxidants and proteases[49–51]. At 90 ℃ produces a bidirectional effect on ECM-receptor interactions. The ECM consists of a complex mixture of structural and functional macromolecules with roles in tissue and organ morphogenesis. Integrins and proteoglycans, such as CD36, allow control of cellular activities, such as adhesion, migration, differentiation, proliferation and apoptosis[52–53]. Such interactions may suppress the action of dystroglycan, reducing risk of viral myocarditis and hypertrophic right ventricular cardiomyopathy and hypertrophic cardiomyopathy. Protein function was severely reduced after at 120 ℃ and proteins with roles in transcriptional misregulation in cancer, proteoglycans in cancer, asthma, SLE, rheumatoid arthritis, primary immunodeficiency, dilated cardiomyopathy and other pathways were upregulated. Proteins involved in proteasome, Ras signaling pathway, cAMP signaling pathway, oocyte meiosis, endocytosis, AMPK signaling pathway, adrenergic signaling in cardiomyocytes, TGF-β signaling pathway, axon regeneration and tight junctions were all down-regulated. While using proteomics for predicting protein function, proteins are first digested in the gastrointestinal tract and it is a question to ponder whether these changes will also make a difference in the digest.

5 Conclusion

Protein functional changes are related to structural changes caused by heat treatment. Oxidation of yak milk proteins with increasing temperature of results in structural and functional changes. Sixty-two proteins decreased and 49 increased at 65 ℃, 31 decreased and 37 increased 90 ℃ and 327 decreased and 308 increased at 120 ℃. Biological processes, cellular components and molecular functions were all affected. Higher temperatures led to more severe disruption of protein function with 4 pathways upregulated and 7 downregulated at 65 ℃, 5 upregulated and 4 downregulated at 90 ℃ and 11 upregulated and 33 downregulated at 120 ℃. At 65 ℃, oxidative phosphorylation and Hedgehog signaling were upregulated and SLE and prion disease downregulated. At 90 ℃, transcriptional misregulation in cancer, gastric cancer and arrhythmogenic right ventricular cardiomyopathy were upregulated and glycosaminoglycan degradation and EGFR tyrosine kinase inhibitor resistance downregulated. PI3K-Akt signaling pathway, ECM-receptor interaction and small cell lung cancer pathways were either reduced or increased. At 120 ℃, glycolysis/gluconeogenesis, transcriptional misregulation in cancer and primary immunodeficiency were upregulated and oxidative phosphorylation, insulin signaling pathway, parathyroid hormone synthesis, Ras signaling pathway and cAMP signaling pathway downregulated. Lower temperature treatments achieve better preservation of function for yak milk proteins and conserve the nutritional value. Treatment of yak milk at too high temperature may cause excessive oxidation, reducing nutritional value and having health implications.

Conflicts of interest

There are no conflicts of interest to declare.

Acknowledgement

This work was financially supported by the Natural Science Foundation of China (32160561), Tibetan Academy of Agriculture and Animal Husbandry-Northwest Agriculture and Forestry University Joint Project (XNLH2022-03), Graduate Research and Innovation Project of Tibet Agriculture & Animal Husbandry University (YJS2022-34) and National Key R&D Program Project (2018YFD0400102).

Author contributions

Formal analysis, Wenhan Wang; Funding acquisition, Rong Jing; Project administration, Sengbiao Shu; Software, Jie Yang; Writing-original draft, Jinchao Zhang; Writing-review & editing, Yu Zhang; Liang Li, Zhendong Liu.

References

[1] M. Ajmal, M. Nadeem, M. Imran, et al., Lipid compositional changes and oxidation status of ultra-high temperature treated milk, Lipids Health Dis. 17 (2018) 227. https://doi.org/10.1186/s12944-018-0869-3.

[2] F. Mahmoodani, C. O. Perera, G. Abernethy, et al., Lipid oxidation and vitamin D_3 degradation in simulated whole milk powder as influenced by processing and storage, Food Chem. 261 (2018) 149–156. https://doi.org/10.1016/j.foodchem.2018.04.043.

[3] C. B. Afonso, C. M. Spickett, Lipoproteins as targets and markers of lipoxidation, Redox Biol. 23 (2019) 101066. https://doi.org/10.1016/j.redox.2018.101066.

[4] J. H. Kim, H. J. Lee, D. M. Shin, et al., The dry-aging and heating effects on protein characteristics of beef *longissiumus dorsi*, Korean J. Food Sci. Anim. Resour. 38(5) (2018) 1101–1108. https://doi.org/10.5851/kosfa.2018.e43.

[5] R. T. Dean, S. Fu, R. Stocker, et al., Biochemistry and pathology of radical-mediated protein oxidation, Biochem. J. 324(1) (1997) 1–18. https://doi.org/10.1006/abbi.1997.9982.

[6] A. Aicardo, M. Mastrogiovanni, A. Cassina, et al., Propagation of free-radical reactions in concentrated protein solutions, Free Radic. Res. 2018, 52(2): 159–170. https://doi.org/10.1080/10715762.2017.1420905.

[7] W. G. Sun, W. L. Xu, H. K. Liu, et al., γ-Tocotrienol induces mitochondria-mediated apoptosis in human gastric adenocarcinoma SGC-7901 cells, J. Nutr. Biochem. 20(4) (2009) 276–284. https://doi.org/10.1016/j.jnutbio.2008.03.003.

[8] J. Y. Zhang, Y. L. Zhao, Y. T. Ding, et al., Relationships of lipid oxidation and protein oxidation with flavor characteristics of meat products, J. Nuclear Agri. Sci. 32(7) (2018) 1417–1424. https://doi.org/10.11869/j.issn.100-8551.2018.07.1417.

[9] A. B. Gurung, A. Bhattacharjee, Impact of tyrosine nitration at positions Tyr307 and Tyr335 on structural dynamics of lipoprotein-associated phospholipase A_2–A therapeutically important cardiovascular biomarker for atherosclerosis, Int. J. Biol. Macromol. (2018) 1956–1964. https://doi.org/10.1016/j.ijbiomac.2017.10.068.

[10] I. Majkutewicz, E. Kurowska, M. Podlacha, et al., Age-dependent effects of dimethyl fumarate on cognitive and neuropathological features in the streptozotocin-induced rat model of Alzheimer's disease, Brain Res. 1686 (2018) 19–33. https://doi.org/10.1016/j.brainres.2018.02.016.

[11] A. L. Bulteau, N. P. Mena, F. Auchère, et al., Dysfunction of mitochondrial Lon protease and identification of oxidized protein in mouse brain following exposure to MPTP: implications for Parkinson disease, Free Radic. Biol. Med. 108 (2017) 236–246. https://doi.org/10.1016/j.freeradbiomed.2017.03.036.

[12] Z. L. Li, Y. H. Shi, Y. Y. Ding, et al., Dietary oxidized tyrosine (O-Tyr) stimulates TGF-β1-induced extracellular matrix production via the JNK/p38 signaling pathway in rat kidneys, Amino Acids 49(2) (2017) 241–260. https://doi.org/10.1007/s00726-016-2353-6.

[13] A. H. Bryk, M. Konieczynska, P. Rostoff, et al., Plasma protein oxidation as a determinant of impaired fibrinolysis in type 2 diabetes, Thromb. Haemost. 119(2) (2019) 213–222. https://doi.org/10.1055/s-0038-1676609.

[14] Y. H. Yang, H. Zhang, B. Yan, et al., Health effects of dietary oxidized tyrosine and dityrosine administration in mice with nutrimetabolomic strategies, J. Agric. Food Chem. 65(32) (2017) 6957–6971. https://doi.org/10.1021/acs.jafc.7b02003.

[15] Y. Y. Ding, X. R. Cheng, Z. Q. Li, et al., Effect of dietary oxidized tyrosine products on insulin secretion via the oxidative stress-induced mitochondria damage in mice pancreas, RSC Adv. 7(43) (2017) 26809–26826. https://doi.org/10.1039/c7ra02945d.

[16] Y. Y. Ding, Z. Q. Li, X. R. Cheng, et al., Dityrosine administration induces dysfunction of insulin secretion accompanied by diminished thyroid hormones T3 function in pancreas of mice, Amino Acids 49 (2017) 1401–1414. https://doi.org/10.1007/s00726-017-2442-1.

[17] Y. Y. Ding, X. Tang, X. R. Cheng, et al., Effects of dietary oxidized tyrosine products on insulin secretion via the thyroid hormone T3-regulated TRβ1-Akt-mTOR pathway in the pancreas, RSC Adv. 7(86) (2017) 54610–54625. https://doi.org/10.1039/C7RA10435A.

[18] J. Lu, X. Y. Wang, W. Q. Zhang, et al., Comparative proteomics of milk fat globule membrane in different species reveals variations in lactation and nutrition, Food Chem. 196 (2016) 665–672. https://doi.org/10.1016/j.foodchem.2015.10.005.

[19] J. Lu, S. Zhang, L. Liu, et al., Comparative proteomics analysis of human and ruminant milk serum reveals variation in protection and nutrition, Food Chem. 261 (2018) 274–282. https://doi.org/10.1016/j.foodchem.2018.04.065.

[20] X. P. Chang, J. M. Zhang, Z. D. Liu, et al., Integrated proteomic, phosphoproteomic, and *N*-glycoproteomic analyses of the *longissimus thoracis* of yaks, Curr. Res. Food Sci. 5 (2022) 1494–1507. https://doi.org/10.1016/j.crfs.2022.09.012.

[21] J. Xiao, J. Q. Wang, R. Y. Gan, et al., Quantitative *N*-glycoproteome analysis of bovine milk and yogurt, Curr. Res. Food Sci. 5 (2022) 182–190. https://doi.org/10.1016/j.crfs.2022.01.003.

[22] W. K. Kim, A. Henschel, C. Winter, et al., The many faces of protein-protein interactions: a compendium of interface geometry, PLoS Comput. Biol. 2(9) (2006) e124. https://doi.org/10.1371/journal.pcbi.0020124.

[23] L. Zhang, S. Boeren, J. A. Hageman, et al., Bovine milk proteome in the first 9 days: protein interactions in maturation of the immune and digestive system of the newborn, PLoS ONE 10(2) (2015) e0116710. https://doi.org/10.1371/journal.pone.0116710.

[24] F. Mestdagh, B. Kerkaert, T. Cucu, et al., Interaction between whey proteins and lipids during light-induced oxidation, Food Chem. 126(3) (2011) 1190–1197. https://doi.org/10.1016/j.foodchem.2010.11.170.

[25] Y. H. Shao, Z. T. Gan, E. Epifanovsky, et al., Advances in molecular quantum chemistry contained in the Q-Chem 4 program package, Mol. Phys. 113(2) (2014) 184–215. https://doi.org/10.1080/00268976.2014.952696.

[26] Y. G. Cao, A. D. True, J. Chen, et al., Dual role (anti- and pro-oxidant) of gallic acid in mediating myofibrillar protein gelation and gel *in vitro* digestion, J. Agric. Food Chem. 64(15) (2016) 3054–3061. https://doi.org/10.1021/acs.jafc.6b00314.

[27] R. J. Wang, R. N. Wang, X. Y. Niu, et al., Role of astrocytes-derived *D*-serine in PFOS-induced neurotoxicity through NMDARs in the rat primary hippocampal neurons, Toxicology 422 (2019) 14–24. https://doi.org/10.1016/j.tox.2019.04.007.

[28] K. Kieserling, T. M. Vu, S. Drusch, et al., Impact of pectin-rich orange fibre on gel characteristics and sensory properties in lactic acid fermented yoghurt, Food Hydrocoll. 94 (2019) 152–163. https://doi.org/10.1016/j.foodhyd.2019.02.051.

[29] L. Li, L. Shi, S. D. Yang, et al., SIRT7 is a histone desuccinylase that functionally links to chromatin compaction and genome stability, Nature Commun. 7 (2016) 12235. https://doi.org/10.1038/ncomms12235.

[30] Y. P. Du, T. X. Cai, T. T. Li, et al., Lysine malonylation is elevated in type 2 diabetic mouse models and enriched in metabolic

associated proteins, Mol. Cell. Proteomics 14(1) (2015) 227–236. https://doi.org/10.1074/mcp.M114.041947.

[31] C. Song, Y. B. Liu, R. Fontana, et al., Elimination of unaltered DNA in mixed clinical samples via nuclease-assisted minor-allele enrichment, Nucleic Acids Res. 44(19) (2016) e146. https://doi.org/10.1093/nar/gkw650.

[32] D. Zhao, S. W. Zou, Y. Liu, et al., Lysine-5 acetylation negatively regulates lactate dehydrogenase A and is decreased in pancreatic cancer, Cancer Cell. 23(4) (2013) 464–476. https://doi.org/10.1016/J.CCR.2013.02.005.

[33] X. Y. Ye, X. M. Niu, L. P. Gu, et al., Desuccinylation of pyruvate kinase M2 by SIRT5 contributes to antioxidant response and tumor growth, Oncotarget 8(4) (2016) 6984–6993. https://doi.org/10.18632/oncotarget.14346.

[34] M. Chevion, E. Berenshtein, E. R. Stadtman, Human studies related to protein oxidation: protein carbonyl content as a marker of damage, Free Radic Res. 33 (2000) S99–S108.

[35] M. Hamada, S. Ishizaki, T. Nagai, Variations of SH content and kamaboko-gel forming ability of shark muscle proteins by electrolysis, 42(3) (1994) 131–135.

[36] F. Li, B. Wang, Q. Liu, et al., Changes in myofibrillar protein gel quality of porcine *longissimus* muscle induced by its stuctural modification under different thawing methods, Meat Sci. 147 (2019) 108–115. https://doi.org/10.1016/j.meatsci.2018.09.003.

[37] R. Lametsch, J. Knudsen, P. Ertbjerg, et al., Therkildsen, novel method for determination of myofibril fragmentation post-mortem, Meat Sci. 75(4) (2007) 719–724. https://doi.org/10.1016/j.meatsci.2006.10.002.

[38] Z. Ceylan, G. F. U. Sengor, O. Sağdıç, et al., A novel approach to extend microbiological stability of sea bass (*Dicentrarchus labrax*) fillets coated with electrospun chitosan nanofibers, LWT-Food Sci. Technol. 79 (2017) 367–375. https://doi.org/10.1016/j.lwt.2017.01.062.

[39] M. Estévez, C. J. C. R. I. F. S. Luna, Nutrition, Dietary protein oxidation: a silent threat to human health?, Crit. Rev. Food Sci. Nutr. 57(17) (2017) 3781–3793. https://doi.org/10.1080/10408398.2016.1165182.

[40] E. Çarkcioğlu, A. J. Rosenthal, K. Candoğan, Rheological and textural properties of sodium reduced salt soluble myofibrillar protein gels containing sodium tri-polyphosphate, J. Texture Stud. 2016. https://doi.org/10.1111/jtxs.12169.

[41] I. A. Jaffe, Adverse effects profile of sulfhydryl compounds in man, Am. J. Med. 80(3) (1986) 471–476. https://doi.org/10.1016/0002-9343(86)90722-9.

[42] F. Hatahet, L. W. Ruddock, R. Signaling, Protein disulfide isomerase: a critical evaluation of its function in disulfide bond formation, Antioxid. Redox Signal. 11(11) (2019) 2807–2850. https://doi.org/10.1089/ars.2009.2466.

[43] S. Bette, H. Breer, J. Krieger, et al., Probing a pheromone binding protein of the silkmoth *Antheraea* polyphemus by endogenous tryptophan fluorescence, Insect Biochem. Mol. Biol. 32(3) (2002) 241–246. https://doi.org/10.1016/S0965-1748(01)00171-0.

[44] W. Z. Sun, F. B. Zhou, D. W. Sun, et al., Effect of oxidation on the emulsifying properties of myofibrillar proteins, Jiangsu J. Agric. Sci. 14(5) (2013) 1703–1712. https://doi.org/10.1007/s11947-012-0823-8.

[45] L. Y. Cai, L. Y. Nian, G. H. Zhao, et al., Effect of herring antifreeze protein combined with chitosan magnetic nanoparticles on quality attributes in red sea bream (*Pagrosomus major*), Food Bioprocess Tech. 12 (2019) 409–421. https://doi.org/10.1007/s11947-018-2220-4.

[46] C. Q. Li, Y. L. Xiong, J. Chen, et al., Oxidation-induced unfolding facilitates myosin cross-linking in myofibrillar protein by microbial transglutaminase, J. Agric. Food Chem. 60(32) (2012) 8020–8027. https://doi.org/10.1021/jf302150h.

[47] G. B. Jameson, J. J. Adams, L. K. Creamer, Flexibility, functionality and hydrophobicity of bovine β-lactoglobulin, Int. Dairy J. 12(4) (2002) 319–329. https://doi.org/10.1016/S0958-6946(02)00028-6.

[48] L. A. Sazanov, P. Hinchliffe, Structure of the hydrophilic domain of respiratory complex I from *Thermus thermophilus*, Science 311 (2006) 1430–1436. https://doi.org/10.1126/science.1123809.

[49] D. Isenberg, A. Rahman, Systemic lupus erythematosus: 2005 annus mirabilis?, Nat. Clin. Pract. Rheumatol. 2(3) (2006) 145–152. https://doi.org/10.1038/ncprheum0116.

[50] C. C. Mok, C. S. Lau, Pathogenesis of systemic lupus erythematosus, J. Clin. Pathol. 56(7) (2003) 481–490. https://doi.org/10.1136/jcp.56.7.481.

[51] H. T. Cook, M. J. N. C. P. R. Botto, Mechanisms of disease: the complement system and the pathogenesis of systemic lupus erythematosus, Nat. Clin. Pract. Rheumatol. 2(6) (2006) 330–337. https://doi.org/10.1038/ncprheum0191.

[52] A. van der Flier, A. Sonnenberg, Function and interactions of integrins, Cell Tissue Res. 305(3) (2001) 285–298. https://doi.org/10.1007/s004410100417.

[53] M. Yepes, TWEAK and Fn14 in the neurovascular unit, Front. Immunol. 4 (2013) 367. https://doi.org/10.3389/fimmu.2013.00367.